

## A Superoxo-Ferrous State in a Reduced Oxy-Ferrous Hemoprotein and Model Compounds

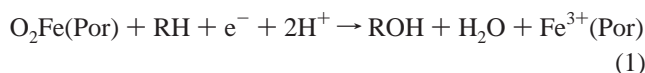
Roman Davydov,<sup>†</sup> James D. Satterlee,<sup>‡</sup> Hiroshi Fujii,<sup>§</sup> Alexandra Sauer-Masarwa,<sup>⊥</sup>  
Daryle H. Busch,<sup>||</sup> and Brian M. Hoffman<sup>\*,†</sup>

Contribution from the Department of Chemistry, Northwestern University, 2156 Sheridan Road, Evanston, Illinois 60208-3113, Department of Chemistry, Washington State University, P.O. Box 644630, Pullman, Washington 99164-4630, Institute for Molecular Science, Myodaiji, Okazaki 444-8585, Japan, and Department of Chemistry, University of Kansas, 1251 Wescoe Hall Drive, 3062 Malott Hall, Lawrence, Kansas 66045-7582

Received July 2, 2003; E-mail: bmh@northwestern.edu

**Abstract:** Cryoreduction of the  $[\text{FeO}_2]^6$  ( $n = 6$  is the number of electrons in 3d orbitals on Fe and  $\pi^*$  orbitals on  $\text{O}_2$ ) dioxygen-bound ferroheme through  $\gamma$  irradiation at 77 K generates an  $[\text{FeO}_2]^7$  reduced oxy-heme. Numerous investigations have examined  $[\text{FeO}_2]^7$  centers that have been characterized as peroxo-ferric centers, denoted  $[\text{FeO}_2]_{\text{per}}^7$ , in which a ferriheme binds a dianionic peroxo-ligand. The generation of such an intermediate can be understood heuristically if the  $[\text{FeO}_2]^6$  parent is viewed as a superoxo-ferric center and the injected electron localizes on the O–O moiety. We here report EPR/ENDOR experiments which show quite different properties for the  $[\text{FeO}_2]^7$  centers produced by cryoreduction of monomeric oxy-hemoglobin (oxy-GMH3) from *Glycera dibranchiata*, which is unlike mammalian “globins” in having a leucine in place of the distal histidine; of frozen aprotic solutions of oxy-ferrous octaethyl porphyrin; and of the oxy-ferrous complex of the heme model, cyclidene. These  $[\text{FeO}_2]^7$  centers are characterized as “superoxo-ferrous” centers ( $[\text{FeO}_2]_{\text{sup}}^7$ ), with nearly unit spin density localized on a superoxo moiety which is end-on coordinated to a low-spin ferrous ion. This assignment is based on their  $g$  tensors and  $^{17}\text{O}$  hyperfine couplings, which are characteristic of the superoxide ion coordinated to a diamagnetic metal ion, and on the absence of detectable ENDOR signals either from the in-plane  $^{14}\text{N}$  ligands or from an exchangeable H-bond proton. Such a center would arise if the electron that adds to the  $[\text{FeO}_2]^6$  superoxo-ferric parent localizes on the Fe ion, to make a superoxo-ferrous moiety. Upon annealing to  $T > 150$  K, the  $[\text{FeO}_2]_{\text{sup}}^7$  species converts to peroxo/hydroperoxo-ferric ( $[\text{FeO}_2\text{H}]^7$ ) intermediates. These experiments suggest that the primary reduction product is  $[\text{FeO}_2]_{\text{sup}}^7$  and that the internal redox transition to  $[\text{FeO}_2]_{\text{per}}^7/[\text{FeO}_2\text{H}]^7$  states is driven at least in part by H-bonding/proton donation by the environment.

In the monooxygenation of substrate (RH) by dioxygen-activating heme enzymes such as cytochromes P450, heme oxygenase (HO), and nitric oxide synthase (NOS), the committed portion of the catalytic cycle begins with one-electron reduction of the enzyme’s oxyferroheme ( $\text{O}_2\text{Fe(P)}$ ) and ends with the hydroxylated product, water, and the ferriheme state:<sup>1</sup>



Such reactions involve one or more of the intermediates in Scheme 1, where we have used the electron-counting procedure introduced to discuss  $[\text{FeNO}]^n$  centers,<sup>2</sup> with  $n$  in the present

case being the sum of electrons in 3d orbitals on Fe and  $\pi^*$  orbitals on  $\text{O}_2$ . Reduction of the  $[\text{FeO}_2]^6$  dioxygen-bound ferroheme generates the  $[\text{FeO}_2]^7$  state; this can react itself or can accept a proton to generate the  $[\text{FeO}_2\text{H}]^7$  hydroperoxoferriheme; again, this species either reacts or accepts a second proton and undergoes heterolytic O–O cleavage to produce Compound I, formally at an Fe(V) valence, but actually containing the  $[\text{Fe(IV)=O}]^{2+}$  ferryl center and a radical.

None of the three enzymic intermediates had been characterized until recently. We began their study through the use of  $\gamma$  irradiation at 4.2–77 K to carry out the first step in Scheme 1, injection into an enzymic  $[\text{FeO}_2]^6$  oxy-ferroheme of the electron that initiates catalysis.<sup>3–5</sup> This creates an  $[\text{FeO}_2]^7$  reduced oxy-heme that is trapped, accessible to study, if the temperature of cryoreduction is sufficiently low. Stepwise annealing to suc-

<sup>†</sup> Northwestern University.

<sup>‡</sup> Washington State University.

<sup>§</sup> Institute for Molecular Science.

<sup>⊥</sup> University of Kansas.

<sup>⊥</sup> Current address: Department of Chemistry, Ben Gurion University, Beer Sheva, 84105, Israel.

(1) Sono, M.; Roach, M. P.; Coulter, E. D.; Dawson, J. H. *Chem. Rev.* **1996**, *96*, 2841–2887.

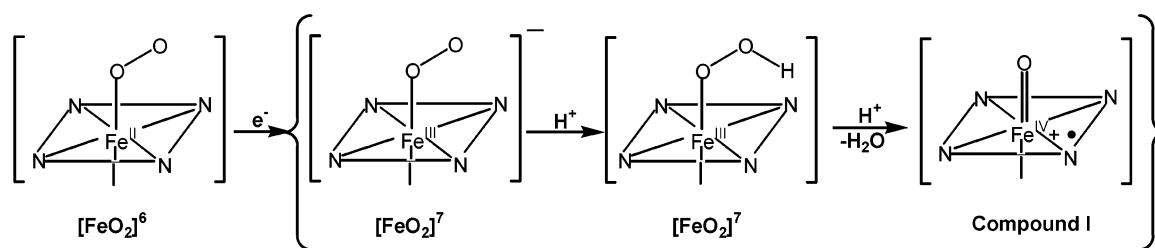
(2) Westcott, B. L.; Enemark, J. H. *Inorg. Electron. Struct. Spectrosc.* **1999**, *2*, 403–450.

(3) Davydov, R.; Ledbetter-Rogers, A.; Martasek, P.; Larukhin, M.; Sono, M.; Dawson, J. H.; Masters, B. S. S.; Hoffman, B. M. *Biochemistry* **2002**, *41*, 10375–10381.

(4) Davydov, R.; Kofman, V.; Fujii, H.; Yoshida, T.; Ikeda-Saito, M.; Hoffman, B. M. *J. Am. Chem. Soc.* **2002**, *124*, 1798–1808.

(5) Davydov, R.; Makris, T. M.; Kofman, V.; Werst, D. W.; Sligar, S. G.; Hoffman, B. M. *J. Am. Chem. Soc.* **2001**, *123*, 1403–1415.

Scheme 1



cessively higher temperatures then advances the enzyme through the successive intermediate stages of its catalytic cycle, all the way to product; a combination of spectroscopic methods, most especially EPR and ENDOR measurements, is used to characterize the catalytic intermediates thus created.

The studies of dioxygen-activating enzymes rest on analogous studies with the dioxygen-carrying proteins, hemoglobin (Hb) and myoglobin (Mb).<sup>6–8</sup> The initial products observed upon 77 K cryoreduction of dioxygen complexes of Hb, Mb, the P450cam D251N mutant, and NOS are similar and have been characterized as  $[\text{FeO}_2]_7$  end-on “ferric-peroxo” species, to be denoted  $[\text{FeO}_2]_{\text{per}}^7$ .<sup>7,9–12</sup> This assignment<sup>6</sup> was based on the observations that the EPR spectra have the unmistakable signature of a low-spin ferriheme species,<sup>13</sup>  $g_1 > g_2 > g_e > g_3$ , in a strong ligand field (small  $g$  dispersion;  $\mathbf{g} \approx [2.24, 2.14, 1.96]$ ). In contrast, the first species to accumulate upon 77 K cryoreduction of oxy-HO and oxy-P450cam is a  $[\text{FeO}_2\text{H}]^7$  hydroperoxo-ferriheme state ( $\mathbf{g} \approx [2.3, 2.18, 1.94]$ ), formed through extraction of a proton from the surroundings by the primary  $[\text{FeO}_2]_7$  product of reduction (Scheme 1).<sup>4,14</sup> Our data clearly confirmed that Compound I is the active hydroxylating intermediate in P450cam,<sup>5</sup> and likely the same holds true for the hydroxylation of L-arginine by NOS.<sup>3</sup> In contrast, we confirmed<sup>4</sup> that  $[\text{FeO}_2\text{H}]^7$  hydroperoxo-ferric form is the reactive heme species that self-hydroxylates in HO.<sup>15</sup> Computational studies such as those by Harris<sup>16</sup> and Loew,<sup>17</sup> Shaik and co-workers,<sup>18</sup> and more recently by Guallar et al.<sup>19</sup> have investigated the energetics of this catalytic mechanism.<sup>20,21</sup>

The generation of an  $[\text{FeO}_2]_{\text{per}}^7$  intermediate upon reduction of  $[\text{FeO}_2]_6$  can be rationalized heuristically if one views the parent oxy-ferrous center of Scheme 1 as being represented by

a “ferric-superoxo” electronic configuration, and that the electron injected by cryoreduction localizes on the O–O moiety to form a dianionic peroxo-ligand bound to the ferriheme. <sup>14</sup>N ENDOR spectra of cryoreduced oxy-Hb, Mb,<sup>22</sup> and P450cam<sup>5</sup> support the assigned  $[\text{FeO}_2]_{\text{per}}^7$  configuration by showing signals from the pyrrole-nitrogen ligands that have hyperfine and quadrupole couplings that are typical of ferrihemes.<sup>5,23,24</sup> Consistent with this configuration, direct measurements show that the spin density on the O–O fragment is small: the <sup>17</sup>O hyperfine splittings seen when <sup>17</sup>O<sub>2</sub> is used exhibit a relatively small coupling from the O atom coordination to Fe,  $A_{\text{max}} = A(g_3) \approx 25$  G, and an undetectably small amount on the remote oxygen,<sup>8,22</sup> in contrast to  $A_{\text{max}} = 76$  G for each O atom in a superoxide ion with unit spin density.<sup>25</sup> <sup>1</sup>H ENDOR spectra of such centers invariably show that they are stabilized by an H-bond that is formed initially to stabilize the parent  $[\text{FeO}_2]_6$  oxyferro-heme.<sup>3,5,8,22</sup>

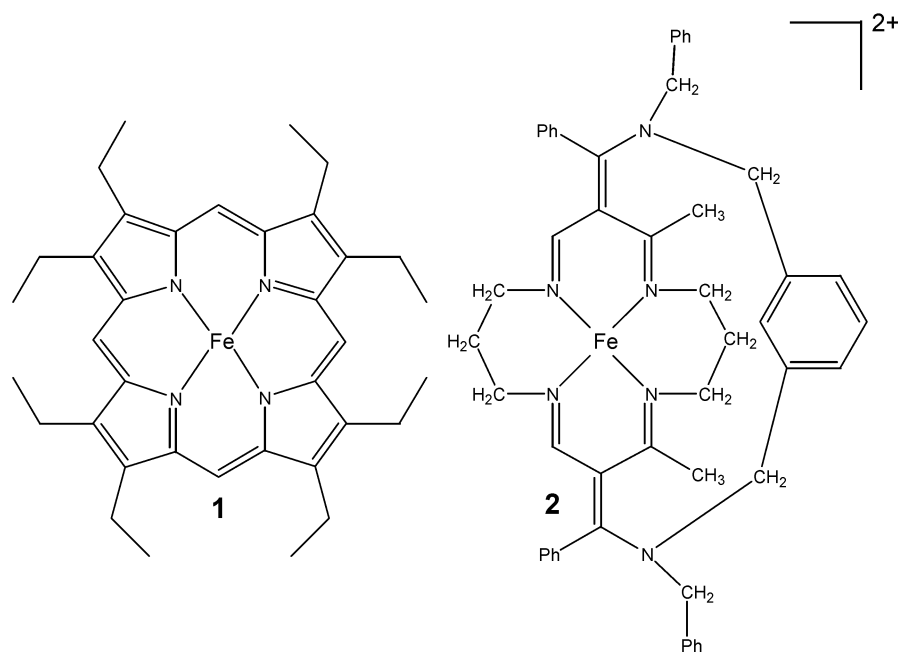
Annealing the  $[\text{FeO}_2]_7$  peroxo-ferriheme centers in Hb, Mb, and the isolated Hb chains to a temperature of ca. 200 K converts them to the  $[\text{FeO}_2\text{H}]^7$  hydroperoxy-ferric-protein complex,<sup>6,8,14,22</sup> while the hydroperoxy-ferric form is the initial product observed upon 77 K cryoreduction of HO and WT P450cam.<sup>4,5</sup> This  $[\text{FeO}_2\text{H}]^7$  center is identified by its larger  $g$ -spread ( $\mathbf{g} \approx [2.30, 2.18, 1.94]$ ),<sup>3–6,8</sup> with principal values, particularly  $g_1$ , that match those for authentic alkylperoxo<sup>26</sup> and hydroperoxo<sup>27,28</sup>-ferriheme complexes. The hydroperoxo-ferriheme center exhibits no resolved <sup>17</sup>O hyperfine couplings,<sup>4,8,22</sup> as would be expected because the formation of the O–H bond creates a hydroperoxo anion that is incapable of effective  $\pi$  delocalization and further drives electron spin from O<sub>2</sub> to Fe.<sup>29</sup> Consistent with this picture, the OH proton of  $[\text{FeO}_2\text{H}]^7$  has a significantly smaller isotropic interaction than the H-bond proton of  $[\text{FeO}_2]_{\text{per}}^7$ , reflecting the diminished spin density on the hydroperoxy moiety; the <sup>14</sup>N hyperfine coupling is correspondingly increased in the hydroperoxo-ferriheme configuration, also consistent with this picture.<sup>5,22</sup> Thus, while the peroxo- and hydroperoxo-ferrihemes are broadly similar, they show distinct and reproducible differences in numerous protein environments.

The assignment of a peroxo-ferriheme electronic configuration to the  $[\text{FeO}_2]_7$  cryoreduction product, with its similarity to the

- (6) Symons, M. C. R.; Petersen, R. L. *Proc. R. Soc. London, Ser. B* **1978**, *201*, 285–300.
- (7) Davydov, R. M. *Biofizika* **1980**, *25*, 203–207.
- (8) Kappl, R.; Höhn-Berlage, M.; Hüttermann, J.; Bartlett, N.; Symons, M. C. R. *Biochim. Biophys. Acta* **1985**, *827*, 327–343.
- (9) In the absence of a strong axial ligand, a third alternative is observed, in which the electron localizes on O–O and generates a side-on ( $\eta^2$ ) ferric-peroxo form characterized by a rhombic high-spin, “ $g$ -4.3” signal; however, this is not observed in metalloproteins, which invariably provide a strong proximal ligand.
- (10) Burstyn, J. N.; Roe, J. A.; Miksztal, A. R.; Shaevitz, B. A.; Lang, G.; Valentine, J. S. *J. Am. Chem. Soc.* **1988**, *110*, 1382–1387.
- (11) Dolphin, D.; Sams, J. R.; Tsin, T. B.; Wong, K. L. *J. Am. Chem. Soc.* **1976**, *98*, 6970–6975.
- (12) McCandlish, E. F. K.; Michael, T. K.; Neal, J. A.; Lingafelter, E. C.; Rose, J. J. *Inorg. Chem.* **1978**, *17*, 1383–1394.
- (13) Walker, F. A. *Coord. Chem. Rev.* **1999**, *186*, 471–534.
- (14) Davydov, R. M.; Yoshida, T.; Ikeda-Saito, M.; Hoffman, B. M. *J. Am. Chem. Soc.* **1999**, *121*, 10656–10657.
- (15) Ortiz de Montellano, P. R. *Acc. Chem. Res.* **1998**, *31*, 543–549.
- (16) Harris, D. L. *J. Inorg. Biochem.* **2002**, *91*, 568–585.
- (17) Harris, D. L.; Loew, G. H. *J. Am. Chem. Soc.* **1998**, *120*, 8941–8948.
- (18) Ogliaro, F.; de Visser, S. P.; Cohen, S.; Sharma, P. K.; Shaik, S. *J. Am. Chem. Soc.* **2002**, *124*, 2806–2817.
- (19) Guallar, V.; Baik, M.-H.; Lippard, S. J.; Friesner, R. A. *Proc. Natl. Acad. Sci. U.S.A.* **2003**, *100*, 6998–7002.
- (20) Hoffman, B. M. *Acc. Chem. Res.* **2003**, *36*, 522–529.
- (21) Hoffman, B. *Proc. Natl. Acad. Sci. U.S.A.* **2003**, *100*, 3575–3578.

- (22) (a) Davydov, R.; Kofman, V.; Nocek, J.; Noble, R. W.; Hui, H.; Hoffman, B. M. *Biochemistry*, submitted. (b) Manuscript in preparation.
- (23) Lee, H.-I.; Dexter, A. F.; Fann, Y.-C.; Lakner, F. J.; Hager, L. P.; Hoffman, B. M. *J. Am. Chem. Soc.* **1997**, *119*, 4059–4069.
- (24) Scholes, C. P. In *Multiple Electron Resonance Spectroscopy*; Dorio, M. M.; Freed, J. H., Eds.; Plenum Press: New York, 1979; pp 297–329.
- (25) Chiesa, M.; Giamello, E.; Paganini, M. C.; Sojka, Z.; Murphy, D. M. *J. Chem. Phys.* **2002**, *116*, 4266–4274.
- (26) Tajima, K.; Edo, T.; Ishizu, K.; Imaoka, S.; Funae, Y.; Oka, S.; Sakurai, H. *Biochem. Biophys. Res. Commun.* **1993**, *191*, 157–164.
- (27) Tajima, K.; Oka, S.; Edo, T.; Miyake, S.; Mano, H.; Mukai, K.; Sakurai, H.; Ishizu, K. *J. Chem. Soc., Chem. Commun.* **1995**, 1507–1508.
- (28) Brittain, T.; Baker, A. R.; Butler, C. S.; Little, R. H.; Lowe, D. J.; Greenwood, C.; Watmough, N. *J. Biochem. J.* **1997**, *326*, 109–115.
- (29) Bartlett, N.; Symons, M. C. R. *Biochim. Biophys. Acta* **1983**, *744*, 110–114.

Chart 1



$[\text{FeO}_2\text{H}]^7$  hydroperoxo-ferriheme state, appears to be in contrast to the results of computations by Harris and Loew.<sup>16,17</sup> These calculations focused on the proton addition steps during the reaction of eq 1, in particular, on the addition of the “second” proton to the  $[\text{FeO}_2\text{H}]^7$  hydroperoxo-ferriheme, and thus they did not remark on the fact that the “primary” oxyheme reduction product generated by their computations is not an  $[\text{FeO}_2]_{\text{per}}^7$  peroxoferriheme with spin density localized on Fe, but rather a “superoxo-ferrous” center ( $[\text{FeO}_2]_{\text{sup}}^7$ ) with  $S = 1/2$  and nearly unit spin density on the  $\text{O}_2$  moiety. Such a center would arise if the electron added to the superoxo-ferric  $[\text{FeO}_2]_6^6$  parent localized on the Fe instead of the O–O, and such an electronic configuration would be expected to exhibit the well-known properties characteristic of the superoxide ion<sup>25</sup> and superoxo-complexes of diamagnetic metal ions,<sup>30</sup> including the dioxygen adducts of Co(II) complexes, which contain a  $[\text{CoO}_2]_7^7$  “superoxo-Co(III)” center.<sup>31</sup> In all of these superoxo centers, the unpaired-spin density resides primarily (or exclusively) in a  $\pi^*$  orbital on the dioxygen moiety; as a result, the  $g$  tensor is characterized by the principal values,  $g_1 \gg g_2 \geq g_3 \approx g_e$ . Indeed, Symons suggested, without corroboration from  $^{17}\text{O}$  hyperfine couplings or  $^1\text{H}/^{14}\text{N}$  ENDOR data, that such a species may be formed upon cryoreduction of monomeric oxy-Hb (oxy-GMH3) from *Glycera dibranchiata*,<sup>29</sup> which differs from mammalian Hb and Mb in having a leucine in place of the distal histidine.<sup>32,33</sup>

In the present paper, we report cryoreduction EPR/ENDOR experiments on oxy-GMH3 and on oxy-ferro-octaethyl porphyrin (OEP; **2**) in an aprotic solvent, as well as on the oxy-complex of the heme model, ferro-cyclidene (**1**; Chart 1)<sup>34</sup> in both protic

and aprotic solvents. These experiments show that in fact both  $[\text{FeO}_2]_{\text{per}}^7$  and  $[\text{FeO}_2]_{\text{sup}}^7$  electronic configurations of the  $[\text{FeO}_2]_7^7$  center can be observed, and we have characterized the newly discovered  $[\text{FeO}_2]_{\text{sup}}^7$  center. This center appears to be the primary product of reduction; the  $[\text{FeO}_2]_7^7$  state that actually accumulates for observation is determined in part by the H-bonding/H-donating character of the environment.

## Experimental Section

Monomeric Hb component III (GMH3) was isolated and purified from specimens of *Glycera dibranchiata*, which were purchased from Maine Bait Co., Wiscasset, ME. Five percent of the population was subjected to random taxonomic classification to confirm the species homogeneity of the specimen sample. The three monomer hemoglobin components (II, III, and IV) were isolated in the Fe(III) forms, using a combination of size exclusion chromatography and ion exchange chromatography, as previously described.<sup>33,35</sup> Component III monomer hemoglobin was concentrated in 0.1 M potassium phosphate buffer, pH 6.8, using Amicon pressure ultrafiltration cells, and then frozen in bulk and stored at  $-80^\circ\text{C}$ .

oxy-GMH3 was prepared by reduction of ferri-GMH3 with dithionite, gel chromatography on a Sephadex G-25 column to remove excess reductant, and then air oxygenation and concentration as necessary. Cryoreduction experiments at 77 K employed frozen solutions of  $\sim 1$  mM oxy-GMH3 in 0.1 M KPi, pH 6.8, containing 16% v/v glycerol. oxy( $^{17}\text{O}_2$ )-GMH3 was made by incubation of ferri-GMH3 with  $^{17}\text{O}_2$  gas (80.5 enrichment in  $^{17}\text{O}$ , Isotec). The same buffer/glycerol mixture saturated with  $^{17}\text{O}_2$  was irradiated for comparison.

Fe(II)-1-(Py)<sub>2</sub> was synthesized<sup>11</sup> and oxy-Fe(II)OEP (Py) in DMF was prepared<sup>36</sup> as described. Cl-Fe(II)-2 ( $\text{R}^3 = \text{Ph}$ ,  $\text{R}^2 = \text{Bz}$ , and  $\text{R}^1 = m\text{-xyl}$ ) was synthesized,<sup>37</sup> and dioxygen complexes were prepared<sup>34</sup> as described. Solutions of oxy-2 for cryoreduction were prepared in

(30) Fukuzumi, S.; Ohtsu, H.; Ohkubo, K.; Itoh, S.; Imahori, H. *Coord. Chem. Rev.* **2002**, *226*, 71–80.

(31) Hoffman, B. M.; Diemente, D. L.; Basolo, F. *J. Am. Chem. Soc.* **1970**, *92*, 61–65.

(32) Braden, B. C.; Arents, G.; Padlan, E. A.; Love, W. E. *J. Mol. Biol.* **1994**, *238*, 42–53.

(33) Park, H.-J.; Yang, C.; Treff, N.; Satterlee, J. D.; Kang, C. *Proteins: Struct., Funct., Genet.* **2002**, *49*, 49–60.

(34) Sauer-Masarwa, A.; Herron, N.; Fendrick, C. M.; Busch, D. H. *Inorg. Chem.* **1993**, *32*, 1086–1094.

(35) Teske, J.; Edmonds, C.; Deckert, G.; Satterlee, J. J. *Protein Chem.* **1997**, *16*, 139–150.

(36) Tajima, K. *Chem. Commun.* **1990**, 144–145.

(37) Herron, N.; Zimmer, L. L.; Grzybowski, J. J.; Olszanski, D. J.; Jackels, S. C.; Callahan, R. W.; Cameron, J. H.; Christoph, G. G.; Busch, D. H. *J. Am. Chem. Soc.* **1983**, *105*, 6585–6596.

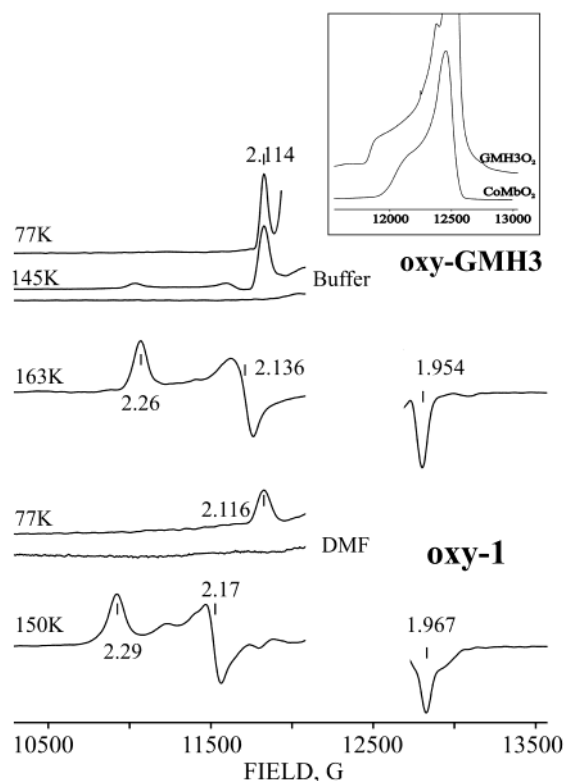


**Figure 1.** EPR spectra of oxy-GMH3 in 16% glycerol/buffer and of oxy-1 in DMF,  $\gamma$ -irradiated at 77 K and after annealing at indicated temperatures. EPR spectra of  $\text{O}_2$ -saturated glycerol/buffer and DMF,  $\gamma$ -irradiated at 77 K, are presented for comparison. Radical signals at  $g \approx 2$  which are induced by irradiation are omitted for clarity; likewise omitted is a weak mixed-valence signal with  $g < 2$  in the oxy-1 spectrum, arising from cryoreduction of a small amount of  $\mu$ -oxo-ferric dimer formed during oxygenation.<sup>44</sup> Conditions:  $T = 2$  K; microwave frequency, 35 GHz; modulation amplitude, 1.5 G.

methanol/1-MeIm (1.5 M), acetone/acetonitrile (2:1)/1-MeIm (1.5 M), and DMF/acetonitrile/1-MeIm (1.5 M).

Cryoreduction at 77 K using a Gammacell 220  $^{60}\text{Co}$  irradiator, annealing protocols, and 35 GHz EPR/ENDOR procedures using rapid-passage techniques have been described.<sup>3–5</sup>

## Results

**oxy-GMH3.** The EPR spectrum of the  $[\text{FeO}_2]^7$  center generated by cryoreduction of oxy-GMH3 does not show a signal corresponding to a ferriheme center, Figure 1, but rather a “ $g$ -parallel” peak at  $g_1 = 2.11$  that is not present in the control spectrum of  $\gamma$ -irradiated solvent saturated with dioxygen. This peak is associated with a species whose additional features are characterized by  $(g_2, g_3) \approx g_e$  and are hidden under the signal from radicals produced during cryo-irradiation, as seen in the absorption-display spectrum in the inset. Such spectra are characteristic of a superoxo species, with  $g_1 \gg g_2 \approx g_3 \approx g_e$ ;<sup>25,30,31</sup> as seen in the inset, the absorption display of the spectrum resembles that for the  $[\text{CoO}_2]^7$  superoxo-Co(III) center of oxy-CoMb (inset, Figure 1). Thus, cryoreduction of the  $[\text{FeO}_2]^6$  oxyferroheme in GMH3 produces a state best described by the alternate  $[\text{FeO}_2]_{\text{sup}}^7$  electronic configuration, in which a superoxo-ion is coordinated to a low-spin ( $d^6$ ;  $S = 0$ ) ferroheme.

The assignment of this feature to a  $[\text{FeO}_2]_{\text{sup}}^7$  center is confirmed, and information about its electronic structure is provided by experiments that use  $^{17}\text{O}_2$  ( $\sim 80\%$   $^{17}\text{O}$ ). We begin with the spectrum of buffer saturated with  $^{17}\text{O}_2$  ( $\sim 80\%$   $^{17}\text{O}$ )

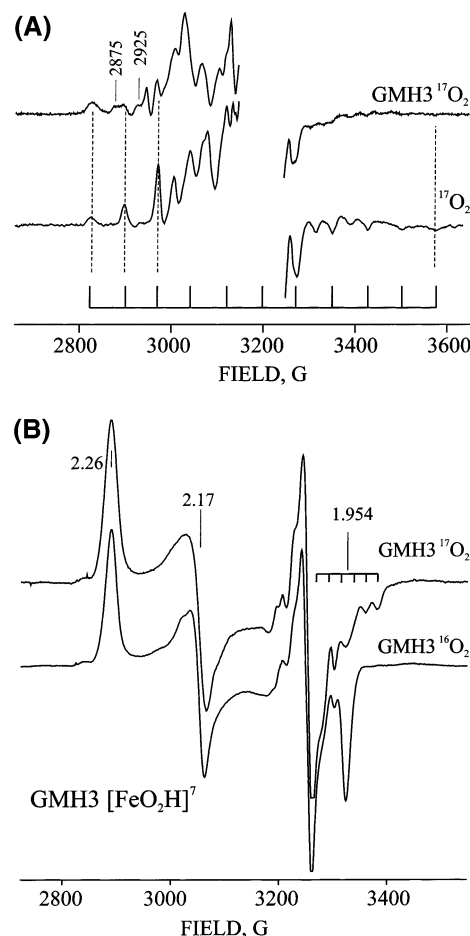


**Figure 2.** (Panel A) EPR spectra of oxy( $^{17}\text{O}_2$ )-GMH3 and glycerol/buffer saturated with  $^{17}\text{O}_2$  (80%  $^{17}\text{O}_2$ ), all  $\gamma$ -irradiated at 77 K. (Panel B) EPR spectra of cryoreduced oxy( $^{17}\text{O}_2$ ) GMH3 and oxy( $^{16}\text{O}_2$ )-GMH3 annealed at 200 K. Conditions:  $T = 77$  K; microwave frequency, 9.1 GHz; modulation amplitude, 5 G.

and cryoreduced at 77 K, Figure 2A. It shows the pattern expected for  $^{17}\text{O}$ -enriched  $\text{O}_2^-$  generated by cryoreduction of  $^{17}\text{O}_2$  in solution;<sup>25</sup> we attribute the absence of any signal for  $^{16}\text{O}_2^-$  in Figure 1 to the fact that the single  $g_1$  peak for  $^{16}\text{O}_2^-$  falls under the radical signals, while the  $^{17}\text{O}$  splittings extend the pattern far outside these signals. The spin density of  $\text{O}_2^-$  is shared equally between the two O atoms, and the two atoms of  $^{17}\text{O}_2^-$  have identical hyperfine tensors; the breadth of the EPR spectrum in Figure 2A is determined by the 11-line pattern from the hyperfine coupling,  $A_3$ , associated with  $g_3 \approx g_e$  from the  $[\text{O}^{17}\text{O}-^{17}\text{O}]^-$  isotopolog, where  $g_3$  lies parallel to the  $2p\pi$  antibonding orbital that contains the unpaired electron. This breadth,  $\Delta = 10A_3 = 750$  G, corresponds to  $A_3 = 75(1)$  G, which equals, within experimental error,  $A_3$  for  $^{17}\text{O}_2^-$  adsorbed on the MgO surface, where<sup>25</sup>  $|A(^{17}\text{O})| = [76.4, 7.2, 8.2]$ .

Next, consider the EPR spectrum obtained from cryoreduced oxy( $^{17}\text{O}_2$ )-GMH3, Figure 2A. The spectrum again is dominated by the 11-line pattern from the solution  $[\text{O}^{17}\text{O}-^{17}\text{O}]^-$ . However, additional features from the  $[\text{Fe}-^{17}\text{O}_2]^7$  center of cryoreduced oxy-GMH3 are clearly observed in the low-field half of the spectrum. In particular, the lowest-field feature of this spectrum, at  $\sim 2875$  G, is assigned as the outermost low-field line from the  $[\text{Fe}-^{17}\text{O}-^{17}\text{O}]_{\text{sup}}^7$  center. With an unsymmetrically bound  $\text{O}_2^-$  moiety, the  $^{17}\text{O}$  hyperfine tensors of the coordinated (c) and remote (r) oxygens need not be the same. In this more

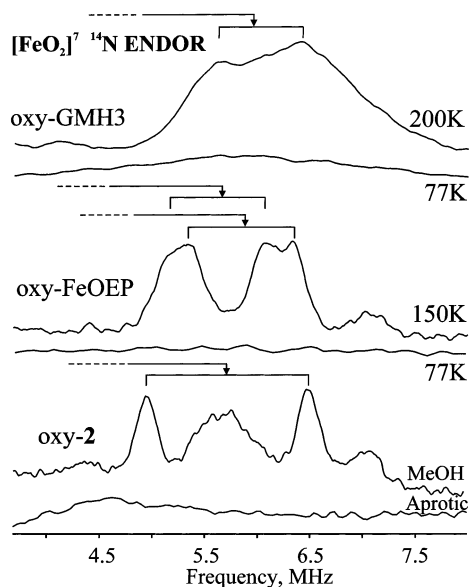


**Figure 3.**  $^{14}\text{N}$  ENDOR spectra taken at  $g_1$  of cryoreduced oxy-GMH3, oxy-1 in DMF, and oxy-2 in MeOH and MeCN/acetone/1-Melm (1.5 M), before and after annealing at indicated temperatures. Conditions:  $T = 2$  K; microwave frequency, 35 GHz; modulation amplitude, 1.5 G; RF power, 10 W; scan speed, 0.2 MHz/s; RF-bandwidth noise broadening of 25 kHz was applied.<sup>45</sup>

general situation, the lowest-field line comes at a field,  $\Delta = 5\bar{A}_3/2$  below the center of the hyperfine pattern,  $B_3 = hv/\beta g_3 \approx hv/\beta g_e$ , where  $\bar{A}_3 = (A_3^c + A_3^r)/2$ . From this feature, we obtain  $\bar{A}_3 \approx 63(3)$  G for oxy( $^{17}\text{O}$ )-GMH3. The lower value of  $\bar{A}_3$  relative to  $A_3$  for the  $\text{O}_2^-$  ion trapped in frozen buffer corresponds to a lower spin density on  $\text{O}_2^-$  bound to the ferriheme. For superoxide with total spin density  $\rho(\text{O}_2) \approx 1$  (50% on each O), each  $^{17}\text{O}$  has a coupling constant,  $A_3 = 75$  G;<sup>25</sup> from this and  $\bar{A}_3$ , one calculates that the  $\text{O}_2$  moiety in the  $[\text{FeO}_2]^7$  center of cryoreduced oxy-GMH3 carries a total spin density,  $\rho(\text{O}_2) \approx 0.83$ . The measurements thus confirm that this species is well-described as a superoxo-ferrous,  $[\text{FeO}_2]_{\text{sup}}^7$ , center.

To proceed, we assign the feature at  $\sim 2925$  G as the next feature in the  $g_3$  pattern. Reflection shows that the separation between this and the outermost (lowest-field) peak corresponds to  $A_3^1 \approx 50$  G for the  $^{17}\text{O}$  with the smaller coupling; we have no evidence as to whether this one is coordinated or remote. From  $A_3^1$  and  $\bar{A}_3$  (defined above), we arrive at the couplings for the two oxygens:  $A_3^1 \approx 50$  G;  $A_3^2 \approx 74$  G, corresponding to a partition of the spin densities on the  $\text{O}_2^-$  fragment  $\rho(\text{O}_2) \approx 0.83$ , into  $\rho^1 \approx 0.3$ ,  $\rho^2 \approx 0.5$ .

As might be expected for a superoxo-[low-spin ( $S = 0$ ) ferrous] electronic configuration,  $^{14}\text{N}$  ENDOR measurements on this  $[\text{FeO}_2]_{\text{sup}}^7$  center show no detectable signals from the pyrrole ligands of Fe (Figure 3).  $^1\text{H}$  ENDOR spectra reveal only signals from nonexchangeable protons with hyperfine couplings of  $A < 5$  MHz, with no strongly coupled exchangeable proton from a hydrogen bond to O–O, Figure 4. Given the high spin density on the superoxo moiety,  $^1\text{H}$  ENDOR would be particularly sensitive to such an interaction, so it is clear that there is no stabilizing H-bond. This is consistent with the absence of an H-bonding distal residue to stabilize oxy-GMH3 and implies there is no H-bond to a bound water, in agreement with EPR and ESEEM studies of oxy-Co-GMH3.<sup>38</sup>

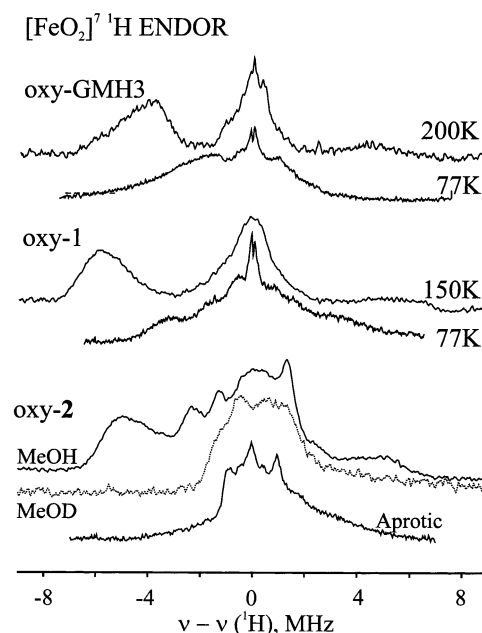


**Figure 4.**  $^1\text{H}$  ENDOR spectra taken at  $g_1$  for 77 K cryoreduced oxy-GMH3, oxy-1 in DMF, and oxy-2 in MeOH, MeOD, and MeCN/acetone, and after annealing at indicated temperatures. Conditions: as in Figure 3, except for a scan speed of 0.5 MHz/s; noise broadening, 60 kHz.

Annealing superoxo-ferro-GMH3 to 145 K eliminates many of the radiation-generated radicals and causes a small fraction of the  $[\text{FeO}_2]_{\text{sup}}^7$  centers to convert to a ferriheme center that corresponds to the  $[\text{FeO}_2]_{\text{per}}^7$  peroxo-ferriheme “electronic isomer”, with  $\mathbf{g} = [2.261, 2.138, 1.956]$ , Figure 1; this conversion is largely complete at 165 K and complete by annealing to 200 K, Figure 1.

Assignment of this conversion to an internal  $\text{Fe} \rightarrow \text{O}_2$  electron transfer is confirmed by the ferriheme EPR spectrum of the system prepared with  $^{17}\text{O}$  ( $\sim 80\%$ ), Figure 2B. It indeed shows resolved  $^{17}\text{O}$  splittings, but only at  $g_3$ , with slight broadening at  $g_1$  and  $g_2$ . The spectrum does not, however, display the 11-line pattern from centers with equivalent coupling to two  $^{17}\text{O}$ – $^{17}\text{O}$  (or more lines for nonequivalent  $^{17}\text{O}$ ). Instead, the  $g_3$  feature is split into a 6-line pattern,  $A_3 \approx 25$  G, from coupling to a single  $^{17}\text{O}$ . This pattern comes from isotopologs in which the oxygen coordinated to Fe is labeled,  $^{17}\text{O}^c$ , which includes both  $[\text{Fe}-^{17}\text{O}-^{17}\text{O}]$  and  $[\text{Fe}-^{17}\text{O}-^{16}\text{O}]$ . There is no resolved coupling to a remote label,  $^{17}\text{O}^r$ ; a residual feature at  $g_3$  arises from  $[\text{Fe}-^{16}\text{O}-^{17}\text{O}]$  and  $[\text{Fe}-^{16}\text{O}-^{16}\text{O}]$ . From this result, we may estimate  $\rho_0^c \approx 0.15$ , with little or no spin density on  $\text{O}^r$ . Hence, ca. 85% of the spin is on the ferriheme, and the center is properly denoted as a  $[\text{FeO}_2]_{\text{per}}^7$  peroxo-ferriheme. This is confirmed by the  $^{14}\text{N}$  ENDOR spectrum of peroxo-ferri-GMH3, which shows signals in the frequency range characteristic of the  $\nu_+$  branch for the pyrrole nitrogens in a typical ferriheme (Figure 3).<sup>5,23,24</sup> The spectrum is not well-resolved, indicative that the well-defined  $[\text{FeO}_2]_{\text{per}}^7$  EPR spectrum from cryoreduced/annealed oxy-GMH3, Figure 1, in fact arises from a ferriheme center that is frozen in multiple conformational substates, a not uncommon observation.<sup>5</sup> Nonetheless, as shown in the figure, features can be assigned to the quadrupole-split  $^{14}\text{N}$  lines, at  $\nu_+(\pm) = A/2 + \nu_N \pm 3P/2$ , from a dominant substate; these

(38) Lee, H. C.; Ikeda-Saito, M.; Yonetani, T.; Magliozzo, R. S.; Peisach, J. *Biochemistry* **1992**, *31*, 7274–7281.

frequencies corresponding to a hyperfine coupling of  $A = 5.2$  MHz and  $3P = 0.8$  MHz, similar to values for the  $[\text{FeO}_2]_{\text{per}}^7$  state in P450cam(D251N)<sup>5</sup> and mammalian Hb, Mb.<sup>22b</sup>

ENDOR spectra of the  $[\text{FeO}_2]_{\text{per}}^7$  peroxo-ferri-GMH3 also disclose a signal from an exchangeable H-bond proton with hyperfine coupling,  $A(g_1) \approx 12$  MHz, Figure 4. The distal pocket of GMH3 is essentially devoid of amino acids whose side chains provide H-bonding groups, so the appearance of this signal likely indicates that the heme pocket incorporates a water molecule in this state and that this provides a stabilizing H-bond. Neither ferro-GMH3 nor cyanoferri-GMH3 contain heme-pocket water molecules,<sup>33</sup> and the  $^1\text{H}$  ENDOR data for the “daughter”  $[\text{FeO}_2]_{\text{sup}}^7$  show that the dioxygen moiety of the “parent”  $[\text{FeO}_2]_{\text{per}}^6$  oxy-ferro-GMH3 does not experience a stabilizing H-bond. Thus, it would appear that a water molecule enters the heme pocket during annealing. A 2D pattern of  $^1\text{H}$  ENDOR spectra collected across the EPR envelope shows that the principal components and orientations of the hyperfine tensor of the H-bond proton exhibit a range of values (averages ca.  $a_{\text{iso}} \approx 5.3$ ,  $2T \approx 6.6$  MHz), indicating that the position of the putative water is not well-defined. This finding correlates with the conformational heterogeneity indicated by the  $^{14}\text{N}$  ENDOR spectra.

Upon annealing the  $[\text{FeO}_2]_{\text{per}}^7$  centers formed in all other Hb studied and in Mb to a temperature in the vicinity of  $T \lesssim 200$  K, a proton is transferred to the peroxo moiety, generating the  $[\text{FeO}_2\text{H}]^7$  center. In contrast, this conversion does not happen to GMH3 at temperatures as high as  $\sim 240$  K.

**oxy-ferro-OEP (oxy-ferro-1).** The EPR spectrum generated by 77 K cryoreduction of frozen solutions of oxy-ferro-1 in the aprotic solvent, DMF, Figure 1, again is not characteristic of a ferriheme, but shows the  $g_1 = 2.116$  feature of an  $[\text{FeO}_2]_{\text{per}}^7$  superoxo-ferriheme, whose perpendicular components are hidden under the radical signal; cryoreduction of  $\text{O}_2$ -saturated DMF does not produce a detectable superoxide signal, likely because it is lost under the radical signal. This superoxo-ferrous center also does not show an ENDOR signal from the in-plane N4 set of pyrrole ligands, Figure 3. Likewise, there is no stabilizing H-bond to the superoxo moiety, as shown by the absence of a  $^1\text{H}$  ENDOR signal from a strongly coupled exchangeable H-bond proton, Figure 4.

Annealing this species to  $\sim 150$  K converts it directly to the  $[\text{FeO}_2\text{H}]^7$  hydroperoxo-ferri-1 center,<sup>27</sup>  $\mathbf{g} = [2.29, 2.17, 1.967]$ , Figure 1. The  $^{14}\text{N}$  ENDOR spectrum collected at  $g_1$  shows the presence of two distinct types of pyrrole  $^{14}\text{N}$  with slightly different values of  $A$  and  $3P$ :  $A(g_1) = 4.93$  MHz,  $3P(g_1) = 1.0$  MHz,  $A(g_1) = 4.5$  MHz,  $3P(g_1) = 0.9$  MHz. Both the values of the parameters and such a deviation from four-fold symmetry are typical of ferrihemoproteins.<sup>5,23,24</sup> In particular, the value of  $3P$  indicates that  $g_1$  corresponds to the Fe(OEP) normal. An additional peak at  $\nu \approx 7$  MHz is tentatively assigned to the axial Py ligand.

The  $[\text{FeO}_2\text{H}]^7$  center shows a  $^1\text{H}$  ENDOR signal from an exchangeable proton with  $A(g_1) = 13.5$  MHz, quite comparable to the value for the  $[\text{FeO}_2\text{H}]^7$  centers in proteins.<sup>3-5</sup> The hyperfine tensor of this hydroperoxo proton, as determined from a 2D, field-frequency plot of ENDOR spectra, is well-defined, with  $a_{\text{iso}} = 8.3$ ,  $2T = 6.2$  MHz.

**oxy-Fe(II)cyclidene (2).** Oxy-2 was prepared both in protic and in aprotic solvents. Figure 5 presents the EPR spectrum

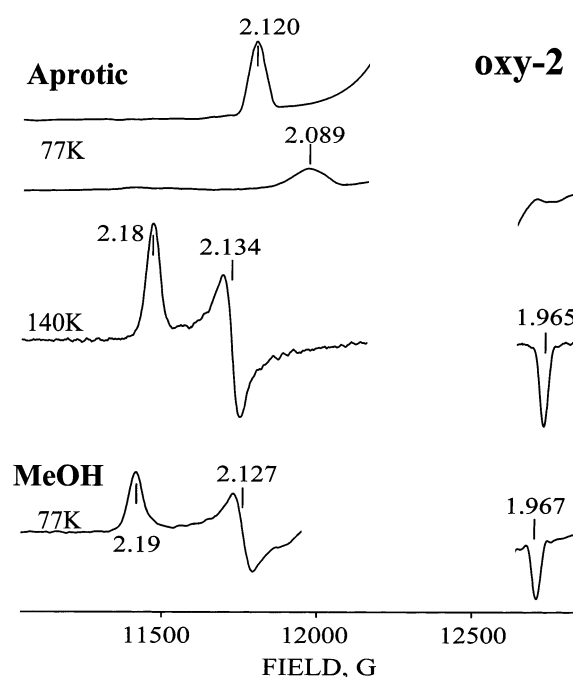


**Figure 5.** EPR spectra of oxy-2 in MeCN/acetone/1-MeIm (1.5 M) and MeOH and MeCN/acetone/1-MeIm (1.5 M) saturated with  $\text{O}_2$ , both  $\gamma$ -irradiated at 77 K and after annealing at indicated temperatures. Conditions are as in Figure 1.

generated by cryoreduction of oxy-2 in the aprotic solvent, MeCN/acetone/1-MeIm. As with oxy-1, the spectrum is that of an  $[\text{FeO}_2]_{\text{per}}^7$  center with the “superoxo-ferrous” configuration, with  $g_1 = 2.12$ . As shown in the figure, superoxide generated from irradiation of  $\text{O}_2$ -saturated solvent shows a signal with  $g_1 = 2.089$ ; this feature is not visible in the spectrum of cryoreduced oxy-2 because the concentration of the Fe complex is high and its signal is intense, while the solution is not saturated with dioxygen and the spectrum from free superoxide is weak. The  $[\text{FeO}_2]_{\text{sup}}^7$  center again shows neither a  $^{14}\text{N}$  ENDOR signal from the in-plane  $^{14}\text{N}$  ligands of cyclidene (Figure 3), nor a  $^1\text{H}$  ENDOR signal from the exchangeable proton of a stabilizing H-bond (Figure 4).

In contrast, the EPR spectrum generated by cryoreduction of oxy-2 dissolved in the protic solvent, MeOH/1-MeIm, Figure 5, is that of the  $[\text{FeO}_2]_{\text{per}}^7$  peroxo/hydroperoxo-ferri-2 center prepared directly by Busch and co-workers.<sup>34,39-41</sup>

By analogy to the cryoreduced centers typically generated from oxy-hemes, the low-spin ferric center generated by cryoreduction of oxy-2 in MeOH could be either the peroxo-ferric or the hydroperoxo-ferric form. Either assignment would require the presence of ENDOR signals from the in-plane  $^{14}\text{N}$  ligands and from an exchangeable proton interacting with the O—O ligand. In fact, strong and sharp  $^{14}\text{N}$  ENDOR signals are detected from the N4 coordination plane of 2. Figure 3 identifies one  $\nu_+$  doublet, with  $A = 4.37$  MHz and  $3P = 1.55$  MHz; two other, broader peaks could be from a second type of ligand  $^{14}\text{N}$  or from axial MeIm. Figure 4 shows a  $^1\text{H}$  ENDOR signal from

(39) Sauer-Masarwa, A.; Dickerson, L. D.; Herron, N.; Busch, D. H. *Coord. Chem. Rev.* **1993**, *128*, 117–137.

(40) When a solution of  $\text{O}_2$ -saturated MeOH is cryoirradiated, as reported by Symons and co-workers, it displays the  $g_1 = 2.08$  signal from superoxide in solution.

(41) Symons, M. C. R.; Stephenson, J. M. *J. Chem. Soc., Faraday Trans. 1* **1981**, *77*, 1579–1583.

a strongly coupled proton associated with this ferri-2 center,  $A(g_1) = 11.5$  MHz, that disappears when the sample is prepared with MeOD as solvent. Preliminary experiments indicate that the hyperfine tensor is well-defined.

When the  $[\text{FeO}_2]_{\text{sup}}^7$  center formed from oxy-2 in the aprotic solvent is annealed to  $\sim 150$  K, its spectrum converts to that of peroxo/hydroperoxo-ferri-2, Figure 5. Presumably, when the frozen solvent glass liquifies during annealing, a water "impurity" is recruited to H-bond/protonate the  $[\text{FeO}_2]^7$  center.

## Discussion

Previous cryoreduction studies of  $[\text{FeO}_2]^6$  oxy-ferro-hemoproteins have yielded two ferriheme product states with nearly unit spin density on the low-spin ferric ion: of these two, the initial product has been characterized as a  $[\text{FeO}_2]_{\text{per}}^7$  peroxo-ferric center; addition of a proton yields the  $[\text{FeO}_2\text{H}]^7$  hydroperoxo-ferric form. The present cryoreduction EPR/ENDOR study of oxy-GMH3, and of model compounds oxy-1 and -2 in aprotic solvent, now establishes the existence of the  $[\text{FeO}_2]_{\text{sup}}^7$  superoxo-ferrous state with high spin density ( $> 80\%$ ) on the "superoxo" moiety. Such a finding was foreshadowed by the incomplete early cryoreduction study of oxy-GMH3,<sup>29</sup> and by computations of Harris<sup>16</sup> and Loew.<sup>17</sup> The cryoreduction/annealing experiments further suggest that the primary reduction product is  $[\text{FeO}_2]_{\text{sup}}^7$  and that the internal redox transition to  $[\text{FeO}_2]_{\text{per}}^7$  is facilitated by environmental stabilization of the latter.

In its stabilization of the  $[\text{FeO}_2]_{\text{sup}}^7$  state upon 77 K cryoreduction, GMH3 is unique among the numerous proteins/enzymes studied to date; in particular, other oxy-Hb's and oxy-Mb all give the  $[\text{FeO}_2]_{\text{per}}^7$  configuration. In GMH3, the distal histidine of the typical "globin" is replaced by leucine, and it would appear that the stability of  $[\text{FeO}_2]_{\text{sup}}^7$  is associated with the absence of an H-bond to the O–O of the parent oxy-GMH3; by comparison with the model compounds 1 and 2, we may say that, in stabilizing the  $[\text{FeO}_2]_{\text{sup}}^7$  configuration, the hydrophobic distal pocket of GMH3 in fact behaves like an aprotic solvent.

Upon annealing cryoreduced oxy-GMH3 to  $\sim 145$ – $160$  K, the distal heme pocket relaxes and the heme center converts to the  $[\text{FeO}_2]_{\text{per}}^7$  configuration. This transition is shown by  $^1\text{H}$  ENDOR measurements to be accompanied by the formation of

an H-bond to the peroxo moiety and may involve the influence of electric field effects. This suggests that the now-charged Fe–O–O moiety recruits a hydrogen-bonding species, most likely a water molecule, from elsewhere in the heme pocket (or outside of it) and that this H-bond then helps induce the "internal electron transfer" associated with the  $[\text{FeO}_2]_{\text{sup}}^7 \rightarrow [\text{FeO}_2]_{\text{per}}^7$  conversion.

Upon annealing GMH3 to yet higher temperatures, the  $[\text{FeO}_2]_{\text{per}}^7$  state persists to  $T \lesssim 240$  K. Again, this differs from the ordinary Hb's and Mb, where annealing an H-bonded  $[\text{FeO}_2]_{\text{per}}^7$  center to a temperature in the vicinity of 200 K leads to the transfer of a proton to the peroxo moiety, generating the  $[\text{FeO}_2\text{H}]^7$  center. Enzymes that split the O–O bond of dioxygen or hydrogen peroxide, such as P450cam, heme oxygenase, and others,<sup>42</sup> appear to differ from the dioxygen-carrying Hb and Mb, in that the former possess a distal-pocket proton-delivery network that protonates the  $[\text{FeO}_2]^7$  center at 77 K or below, such that one observes only the  $[\text{FeO}_2\text{H}]^7$  hydroperoxo-ferriheme.<sup>43,44</sup> During annealing of the  $[\text{FeO}_2]_{\text{sup}}^7$  center generated by reduction of the reduced oxy-1 heme model in aprotic solvent, the center also appears to recruit a proton donor, but it does not "stop" at accepting an H-bond, instead accepting a proton and converting directly to a  $[\text{FeO}_2\text{H}]^7$  hydroperoxo-ferriporphyrin. The  $[\text{FeO}_2]_{\text{sup}}^7$  center formed by reduction of oxy-2 in aprotic solvent also undergoes conversion to a  $[\text{FeO}_2\text{H}]_{\text{per}}^7/[\text{FeO}_2\text{H}]^7$  form upon annealing; current data does not allow discrimination between the peroxo/hydroperoxo forms. In contrast, the 77 K cryoreduction of the oxy-2 model in MeOH directly yields a peroxo/hydroperoxo center.

**Acknowledgment.** We thank Prof. Howard Halpern (Department of Radiation Oncology, Pritzker School of Medicine, University of Chicago) for access to the Gammacell 220  $^{60}\text{Co}$  irradiator. This work was supported by the NIH (HL13531, B.M.H.; GM47645, J.S.; 14340212), the Ministry of Education, Science, Sports, and Culture, Japan (H.F.), and the NSF (D.H.B.).

JA037037E

(42) Unpublished observations.

(43) Only when this network is disrupted, as in the p450cam(D251N) mutant, does the peroxo-ferric form accumulate.

(44) Davydov, R. M.; Smieja, J.; Dikanov, S. A.; Zang, Y.; Que, L., Jr.; Bowman, M. K. *JBIC, J. Biol. Inorg. Chem.* **1999**, *4*, 292–301.